Journal of Power Sources 195 (2010) 2136–2142

Contents lists available at ScienceDirect

Journal of Power Sources

journal homepage: www.elsevier.com/locate/jpowsour

Hydrogen generation from catalytic hydrolysis of alkaline sodium borohydride solution using attapulgite clay-supported Co-B catalyst

Hongjing Tian, Qingjie Guo*, Dongyan Xu

College of Chemical Engineering, Qingdao University of Science & Technology, Key Laboratory of Clean Chemical Processing Engineering of Shandong Province, Qingdao 266042, China

ARTICLE INFO

Article history:
Received 19 August 2009
Received in revised form 2 October 2009
Accepted 2 October 2009
Available online 12 October 2009

Keywords:
Attapulgite clay
Co-B catalyst
Catalytic activity
Recycle ability

ABSTRACT

An attapulgite clay-supported cobalt-boride (Co-B) catalyst used in portable fuel cell fields is prepared in this paper by impregnation–chemical reduction method. The cost of attapulgite clay is much lower compared with some other inert carriers, such as activated carbon and carbon nanotube. Its microstructure and catalytic activity are analyzed in this paper. The effects of NaOH concentration, $NaBH_4$ concentration, reacting temperature, catalyst loadings and recycle times on the performance of the catalysts in hydrogen production from alkaline $NaBH_4$ solutions are investigated. Furthermore, characteristics of these catalysts are carried out in SEM, XRD and TEM analysis. The high catalytic activity of the catalyst indicates that it is a promising and practical catalyst. Activation energy of hydrogen generation using such catalysts is estimated to be 56.32 kJ mol^{-1}. In the cycle test, from the 1st cycle to the 9th cycle, the average hydrogen generation rate decreases gradually from 1.27 l min^{-1} g^{-1} Co-B to 0.87 l min^{-1} g^{-1} Co-B.

1. Introduction

In recent years, the increasing demand for more portable electronic equipments leads to rapid developing of proton exchange membrane (PEM) fuel cells. Although PEM fuel cell is less suited for stationary power generation due to its relatively low thermal efficiency and heavy desire for pure hydrogen fuel [1], it is primarily aimed at the telecommunication market and the transport market. Toshiba [2] prepared to put the new rechargeable battery based on the direct methanol fuel cell (DMFC) technology on electronic markets in 2009. Samsung [2] also announced that they had developed a new military battery with a useful life about 8 times that of ordinary battery and it is expected the new battery will be put on military markets in 2010.

The performance of PEM fuel cell dominantly depends on the stable supply of high purity hydrogen. However, the methods of storing hydrogen using tanks, activated carbon or nanoscale materials cannot keep the long-term hydrogen storage. In addition, when hydrogen is produced from the steam reforming of natural gas, the by-product, carbon monoxide (CO), even a few parts per million, would cause severe inactivation of the catalysts [3]. At present, the borohydrides have been proved as the new stable hydrogen-storage materials. High purity hydrogen can be produced in the self-hydrolysis of the borohydrides. Among them, alkaline sodium borohydride ($NaBH_4$) solution is attracting more attention because it has many advantages, including high theoretical hydrogen content (10.7 wt.%) [4,5], stable self-hydrolysis process, friendliness to the environment, and so on. The self-hydrolysis of $NaBH_4$ in alkaline solution is shown as below:

$$NaBH_4(aq) + 2H_2O \xrightarrow{\text{catalyst}} 4H_2 + NaBO_2(aq), \quad \Delta H^{\theta}_{f,298} = -212.36\ \text{kJ mol}^{-1} \tag{R1}$$

At room temperature, however, the hydrogen generation rate is not satisfactory without the presence of some catalysts. Various catalysts such as Ru catalysts [3,6,7], Pt catalysts [8,9], Pd catalysts [9,10], Ni-B catalysts [11], Co-B catalysts [12,4,13,14], Ni-Co-B catalysts [15], Co-Ni-P catalysts [16,17], Fe-B catalysts [18] have been tested as the catalysts for $NaBH_4$ to accelerate the hydrolysis reaction. Among them, Co-B catalysts are most attractive due to their good catalytic activities and low costs. To realize a well dispersion of these catalysts, they are supported on the surface of some inert carriers, such as activated carbon [10,20] and carbon nanotube [19]. In this paper, a new attapulgite clay-supported Co-B catalyst is developed by the impregnation–reduction method. Attapulgite clay (AT) is fibrillar hydrated magnesium aluminium silicate crystals distributed widely in nature. Its cost is quite low, nearly one-twentieth of activated carbon per ton. Actually it is also a natural nano-structural material. The long and narrow clay particles agglomerate together, forming some fibrous bundles with

* Corresponding author at: College of Chemical Engineering, Qingdao University of Science & Technology, 53 # Zhengzhou Road, Qingdao, Shandong Province, 266042, China. Tel.: +86 0532 84022506; fax: +86 0532 84022757.
E-mail address: qingjieguo@yahoo.cn (Q. Guo).

0378-7753/$ – see front matter.
doi:10.1016/j.jpowsour.2009.10.006

Table 1
Mass losses after the immersing of attapulgite clay particles in alkaline $NaBH_4$ solution.

NaOH concentration (wt.%)	$NaBH_4$ concentration (wt.%)	Temperature (°C)	Soaking time (h)	Mass loss (%)
0	0	40	24	1.95
1	5	25	1	1.75
10	5	25	1	2.38
10	5	40	1	2.16
1	20	25	1	2.51
10	20	25	1	1.67
10	20	40	1	2.36
1	5	25	24	2.21
10	5	25	24	2.09
10	20	40	24	1.84

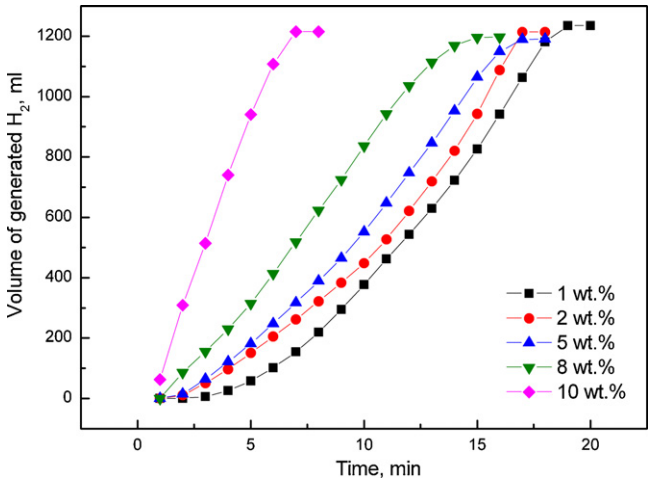

Fig. 1. Effects of NaOH concentration on the hydrogen generation process.

a shape similar to hay bundles. Because of the clay's large surface due to its unique structure, it has an excellent adsorption ability. Furthermore, it has the advantages of resistance to strong acid and alkali corrosion, high temperature endurance and so on. In this paper, the activity of the attapulgite clay-supported Co-B catalysts is investigated. The structures of the catalysts before and after the multi-cycle test are shown, respectively, in SEM and TEM micrographs. Finally, the recyclability of the catalysts is investigated and the activation energy for the hydrolysis reaction is calculated.

2. Experiment

2.1. Catalyst preparation

The attapulgite clay samples (BET surface area of 228.5 $m^2\,g^{-1}$, 300–360 mesh) were obtained from Xuyi of Jiangsu Province in China. Its formula is represented as $Si_8O_{20}(Mg_2Al_{1.4}Fe_{0.31})(OH)_2(OH_2)_4{\cdot}4H_2O$, composed of 62.15 wt.% SiO_2, 10.46 wt.% MgO, 9.25 wt.% Al_2O_3 and 3.26 wt.% Fe_2O_3. Analytical reagent grade sodium borohydride ($NaBH_4$), sodium hydroxide (NaOH) and cobalt nitrate ($Co(NO_3)_2{\cdot}6H_2O$) were used in the catalyst preparation. Firstly, the fresh attapulgite clay samples were calcined at 350 °C in a muffle furnace for 12 h to be dehydrated. Then an aqueous $Co(NO_3)_2$ solution was dripped into 9 g of the clay samples and the mixture was treated in an ultrasonic water bath at a frequency of 40 kHz for 2 h. The product after the dripping was a mushy mixture. After being dried at 90 °C for 12 h, the product was the solid loose catalyst precursors. Subsequently, they were impregnated with 20 ml of 5 wt.% $NaBH_4$ solution to produce the active Co-B compositions. Furthermore, the mixtures were filtered using microporous membrane and immediately washed with distilled water several times. Finally the catalyst samples were dried at 130 °C in a vacuum drying oven for 12 h to eliminate the remaining water molecules. The mass ratio of Co-B loadings was determined to be 10.53 wt.% in the catalysts by measuring the difference between the weights of fresh attapulgite clay samples and the prepared catalysts.

2.2. Stability testing of attapulgite clay

The stability of attapulgite clay in alkaline $NaBH_4$ solution is critical to the catalytic activity of the catalysts. In this experiment,

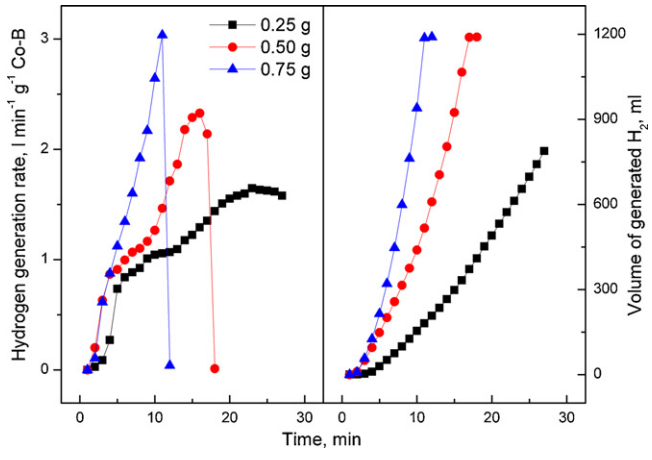

Fig. 2. Effects of the amount of catalysts on the hydrogen generation rate and the volume of generated hydrogen.

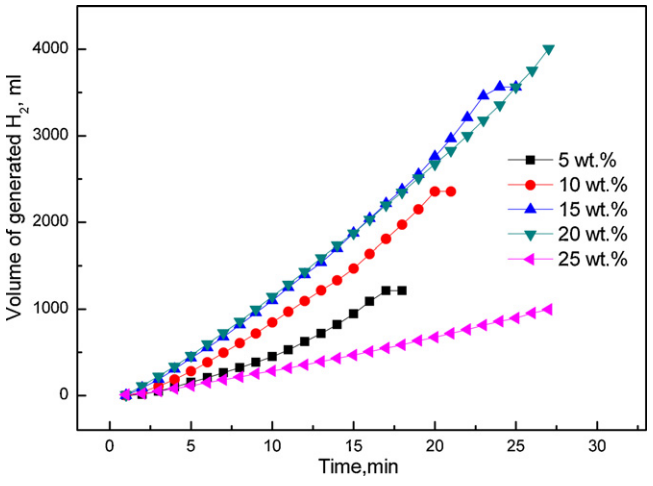

Fig. 3. Effects of $NaBH_4$ concentration on the volume of generated hydrogen.

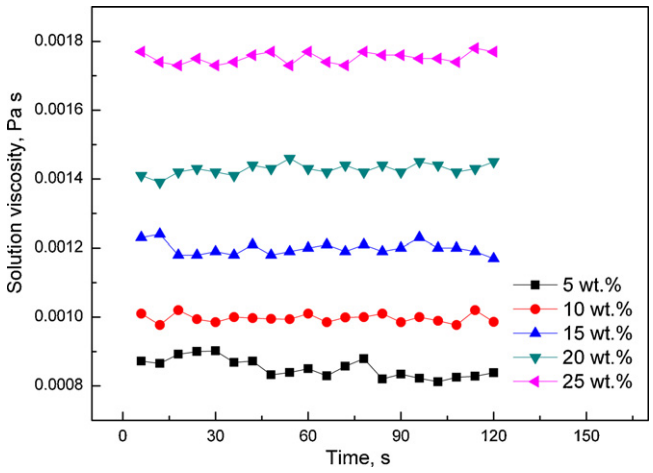

Fig. 4. Effects of $NaBH_4$ concentration on the solution viscosity.

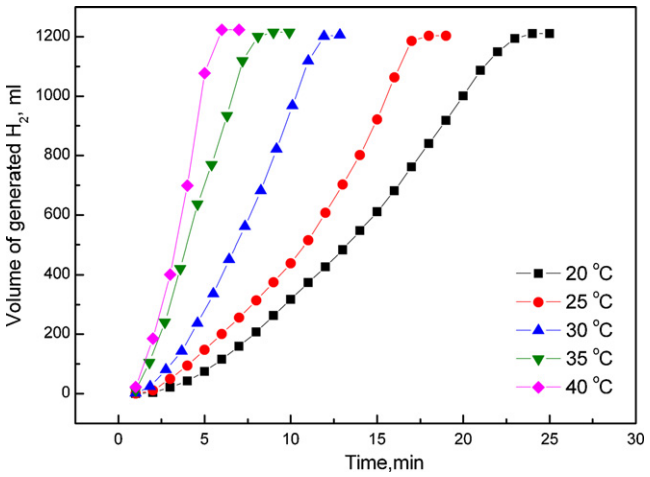

Fig. 5. Effects of reacting temperature on the volume of generated hydrogen.

nine equal parts of dehydrated attapulgite clay were prepared, each being 0.5 g. The samples were put into different alkaline $NaBH_4$ solutions. After being soaked in the solution for some time, the samples were filtered using microporous membrane and washed several times with distilled water. Finally the solid residues were dried at 130 °C in a vacuum drying oven for 12 h and weighed using an analytical balance. The mass losses of each part of the samples were calculated. The results corresponding to different NaOH concentrations, $NaBH_4$ concentrations, reacting temperatures and soaking time are listed in Table 1. To determine what causes the mass losses of the catalysts, the results of the mass losses of the attapulgite clay, before and after soaking in the distilled water, are also listed in Table 1.

It can be seen in Table 1 that the mass losses of the attapulgite clay, after immersing in both the distilled water and the alkaline $NaBH_4$ solution, range from 1.67% to 2.51%. These small values of the samples' mass losses show that the attapulgite clay is a promising stable inert carrier. The slight difference between the values of the samples' mass losses in the distilled water and the alkaline $NaBH_4$ solution indicates that the NaOH concentration and the $NaBH_4$ concentration hardly contribute to the losses of the samples. Considering the attapulgite clay particle is a kind of nanoparticle, the losses of the samples may be caused by some particles escaping through the microporous membrane during the filtration process. In addition, the strong water absorptivity of the attapulgite clay particles causes the close sticking of a large number of clay particles onto the surface of the membrane. Some clay particles may get lost when the samples were removed from the surface of the membrane.

2.3. Performance testing of prepared catalysts

All the hydrogen generation experiments of borohydride hydrolysis in the presence of the catalysts were performed in a 50 ml three-neck round-bottom flask which was immersed in a water bath. One neck is connected with a piece of rubber hose to transfer the evolved hydrogen. The amount of the generated hydrogen was measured by a wet gas flow meter. The middle neck is jammed with a cork. A thermometer is inserted into the solution through the cork to monitor the actual reacting temperature of the solution. The third neck was initially open, but after an immediate supply of prepared catalysts into the solutions using a corundum spoon, it was jammed. Before each test started, the prepared alkaline sodium borohydride solutions were injected into the flask.

3. Results and discussion

3.1. Effects of NaOH concentration

Fig. 1 depicts the effects of NaOH concentration, varying from 1 wt.% to 10 wt.%, on the hydrogen generation process in the presence of 5 wt.% $NaBH_4$ solution and 0.5 g as-prepared catalysts at 25 °C. It can be seen that the reaction time decreases remarkably with an increasing NaOH concentration. When the NaOH concentration keeps at 1 wt.%, the reaction time remains for 25 min. Furthermore, the reaction time reduces sharply to only 7 min when the NaOH concentration increases to 10 wt.%. These findings are consistent with the previous results reported by Ye et al. [21] using

Table 2
Comparison of catalytic properties of catalysts reported in literatures and this paper.

Catalyst	Initial solution temperature (°C)	$NaBH_4$ concentration (wt.%)	NaOH concentration (wt.%)	Catalyst mass (g)	Average hydrogen generation rate ($l\,min^{-1}\,g^{-1}$ catalyst)	Reference
Ru/IRA-400	25	7.5	1	–	0.38	[3]
Ni-Co-B	28	2.7	15	0.10	2.61	[15]
Ni-Ru/50WX8	25	5	5	0.20	0.13	[23]
Co-P	30	10	1	0.20	0.35	[5]
Co-B/MWCNTs	30	20	3	0.01	5.10 ($l\,min^{-1}\,g^{-1}$ Co-B)	[19]
$Co(OH)_2$/AC	25	1	5	0.25	0.53 ($l\,min^{-1}\,g^{-1}$ $Co(OH)_2$)	[14]
$FeCl_3$ solution	–	5	10	3.41	0.32 ($l\,min^{-1}\,g^{-1}$ $FeCl_3$)	[29]
Co/γ-Al_2O_3	30	1	5	0.05	1.11 ($l\,min^{-1}\,g^{-1}$ Co)	[21]
Co-B/AT	25	5	2	0.50	1.42 ($l\,min^{-1}\,g^{-1}$ Co-B)	This work
Co-B/AT	25	5	10	0.50	3.35 ($l\,min^{-1}\,g^{-1}$ Co-B)	This work

Table 3
Comparison of the value of the activated energy in this work with the published values.

Authors	Catalysts	Preparation method	Value of activated energy (kJ mol^{-1})
Jeong et al. [12]	Co-B catalyst	Chemical reduction method	64.87
Ingersoll et al. [15]	Ni-Co-B catalyst	Chemical reduction method	62.00
Eom et al. [5]	Co-P catalyst	Electroless deposition method	60.20
Zhao et al. [20]	Carbon-supported Co-B catalyst	Impregnation–chemical reduction method	57.80
Huang et al. [19]	Multiwalled carbon nanotubes supported Co-B catalysts	Impregnation–chemical reduction method	40.40
Dai et al. [28]	Ni-foam supported Co-B catalyst	Modified electroless plating method	33.00
Liu et al. [23]	Co-B catalyst	Directly adding solid $CoCl_2{\cdot}6H_2O$ into alkaline sodium borohydride solution	52.73
Ye et al. [21]	γ-Al_2O_3 supported Co catalyst	Impregnation–chemical reduction method	32.63
Ye et al. [21]	Activated carbon-supported Co catalyst	Impregnation–chemical reduction method	45.64
Hsueh et al. [25]	Polymer template-Ru catalyst	Chelate formation method	49.72
Zahmakiran and Ozkar [24]	Zeolite-confined Ru(0) nanocluster catalyst	Chemical reduction method	49.00
This work	Attapulgite clay-supported Co-B catalyst	Impregnation–chemical reduction method	56.32

a γ-Al_2O_3 supported Co catalyst, Eom et al. [5] using a Co-P catalyst, Kim et al. [16] using a Co-Ni-P catalyst and Jeong et al. [12] using a Co-B catalyst. However, these results are different from those reported by Metin and Ozkar [22] using a polymer-stabilized cobalt nanoclusters catalyst, Liu et al. [23] using a Ni-Ru nanocomposite catalyst, Liu and Li [4] using a Co-B catalyst, Zahmakiran and Ozkar [24] using a zeolite-confined ruthenium(0) nanocluster catalyst and Hsueh et al. [25] using a polymer template-Ru composite catalyst. Therefore, it is clear that the effects of NaOH concentration on hydrolysis generation rate depend greatly on the type of catalysts. The reason is that the production of Co-B components is a complicated process and is accompanied by some side reactions. The two major side reactions [26] are given below:

$$2Co^{2+} + BH_4^- \rightarrow Co_2B + 0.5H_2 + 3H^+ \quad (R2)$$

$$3H^+ + 3BH_4^- + 9H_2O \rightarrow 3H_3BO_3 + 12H_2 \quad (R3)$$

Therefore, high NaOH concentration could promote the production of active Co-B components but suppress the hydrolysis reaction of sodium borohydride. In addition, it has been reported that high NaOH concentration may result in more production of larger size Co-B particles, which causes low catalytic reactivity of the catalysts [4]. Consequently, for some hydrogen generation process in the presence of Co-B catalyst, there is an optimum range for NaOH concentration to improve the hydrogen generation rate.

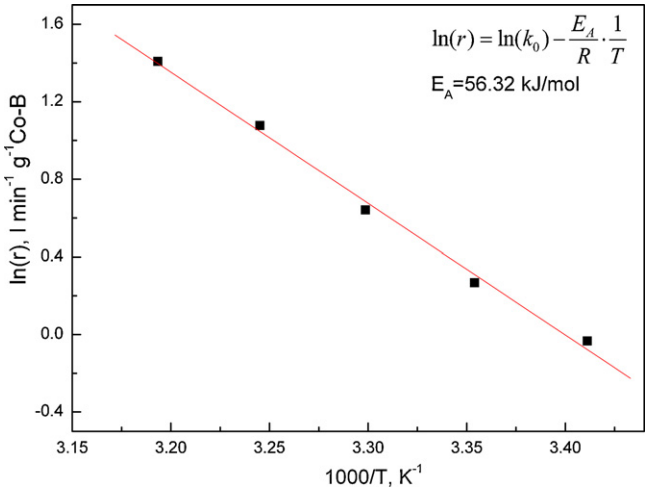

Fig. 6. Arrhenius plot for the hydrogen generation reaction.

3.2. Effects of the amount of catalyst

The effect of the catalyst's amount on the hydrogen generation rate in 5 wt.% $NaBH_4$ + 2 wt.% NaOH solution can be seen in Fig. 2. Obviously, more amount of catalyst greatly improves the hydrogen generation rate and reduces the reaction time. In the presence of 0.25 g catalyst, the hydrogen yield is 800 ml in about 27 min, three-fourths of the theoretical hydrogen yield. The highest

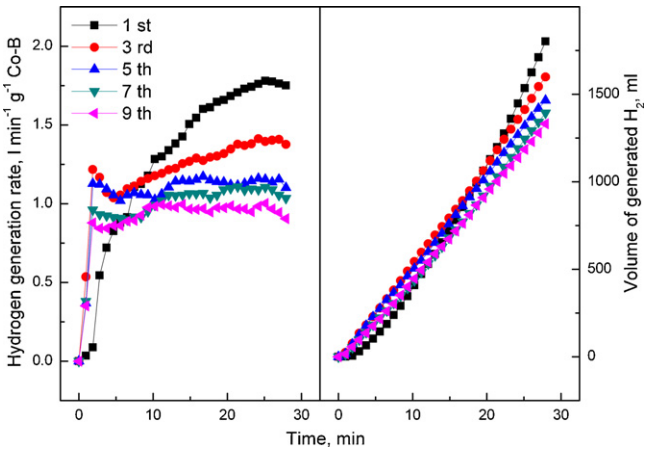

Fig. 7. Effects of recycle time on the volume of generated hydrogen.

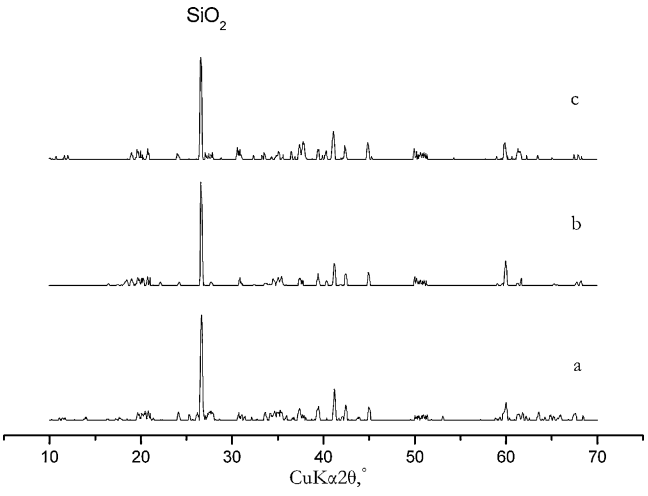

Fig. 8. XRD patterns of (a) the attapulgite clay-supported Co-B catalysts after the 1st recycle test; (b) the catalysts after the 5th recycle test and (c) the catalysts after the 9th recycle test.

hydrogen generation rate is 1.65 l min^{-1} g^{-1} Co-B. When the catalyst's amount increases to 0.75 g, the whole reaction finished in less than 10 min and the actual hydrogen yield approaches the theoretical hydrogen yield. The highest activity achieved is 3.21 l min^{-1} g^{-1} Co-B. Therefore, the hydrogen generation rate could be controlled by adjusting the catalyst amount.

3.3. Effects of $NaBH_4$ concentration

Fig. 3 depicts the effect of $NaBH_4$ concentration on the hydrogen generation rate in the presence of 2 wt.% NaOH solution and 0.5 g catalysts at 25 °C. It can be observed that there is an optimum regime for the $NaBH_4$ concentration to enhance the hydrogen generation rate. As the $NaBH_4$ concentration increases from 5 wt.% to 15 wt.%, the average hydrogen generation rate rises monotonically from 1.42 l min^{-1} g^{-1} Co-B to 2.85 l min^{-1} g^{-1} Co-B. However, when the $NaBH_4$ concentration continues to increase to 25 wt.%, the hydrogen generation rate diminishes significantly to only 0.66 l min^{-1} g^{-1} Co-B. A similar situation is reported by Liu et al. [23] who developed a Ni-Ru nanocomposite catalyst using both the chemical reduction method and the electroless deposition method, Hsueh et al. [25] who prepared a polymer template-Ru composite catalyst using a chelate formation method and Krishnan et al. [27] who developed both a resin bead supported Ru/Pt catalyst using an ion exchange method and a $LiCoO_2$ supported Ru/Pt catalyst using a simple chemical reduction method. Actually, the low hydrogen generation rates corresponding to both low and high $NaBH_4$ concentration can be reasonably attributed to the increase of solution viscosity. Low $NaBH_4$ concentration and high solution viscosity both cause mass-transport limitation of borohydride from the solution to the surface of catalyst. Fig. 4 demonstrates how the $NaBH_4$ concentration affects the solution viscosity at the constant shear rate of 200 s^{-1} for 120 s. The solution viscocity for different $NaBH_4$ concentrations are measured by Rheolab OC rotational viscometer. It can be seen that the solution viscosity maintains nearly constant for a certain level of $NaBH_4$ concentration and high $NaBH_4$ concentration leads to big solution viscosity. When the $NaBH_4$ concentration is 5 wt.%, the solution viscosity is around 8.45E−4 Pa s. The viscosity increases to about 17.45E−4 Pa s when the $NaBH_4$ concentration increases to 25 wt.%. These data are consistent with the findings reported by Amendola et al. [3] and Jeong et al. [12].

A comparison of the hydrogen generation rate of attapulgite clay supported Co-B (Co-B/AT) catalyst with some other published catalysts is given in Table 2. Amendola et al. [3] found that IRA-400 supported Ru catalysts produced an average hydrogen generation rate of 0.38 l min^{-1} g^{-1} catalyst. Ingersoll et al. [15] reported that Ni-Co-B catalysts give an average hydrogen generation rate of 2.61 l min^{-1} g^{-1} catalyst in 2.7 wt.% $NaBH_4$ + 15 wt.% NaOH solution. Liu et al. [23] prepared the Ni-Ru/50WX8 catalyst and discovered it gave an average hydrogen generation rate of 0.13 l min^{-1} g^{-1} catalyst in the presence of 2.7 wt.% $NaBH_4$ + 15 wt.% NaOH solution. Eom et al. [5] performed the experiments on the catalytic activity of

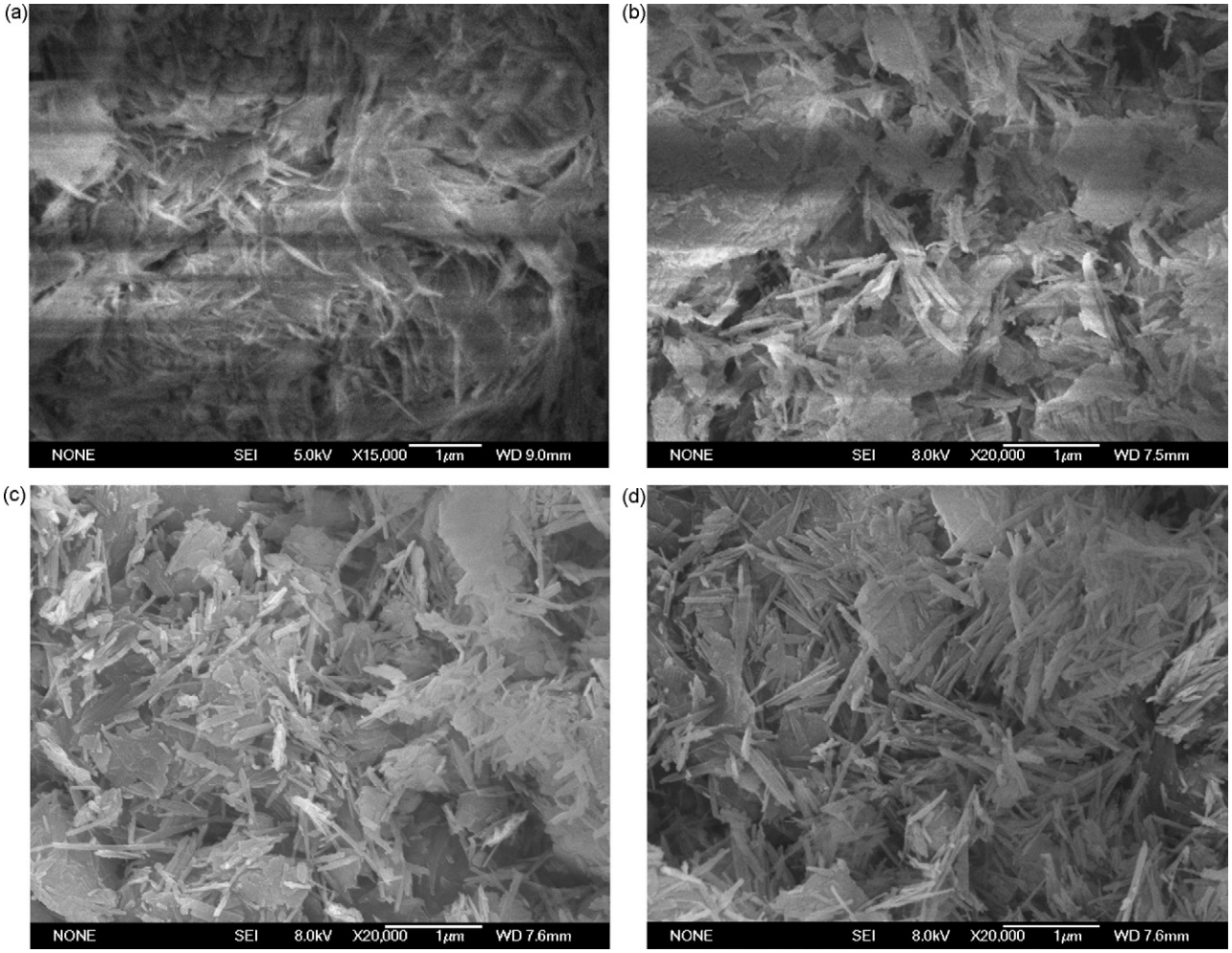

Fig. 9. Scanning electron micrographs of (a) fresh attapulgite clay without supported Co-B catalysts before the recycle test; (b) the catalysts after the 1st recycle test; (c) the catalysts after the 5th recycle test and (d) the catalysts after the 9th recycle test.

Co-P catalysts and found it produced an average hydrogen generation rate of 0.35 l min^{-1} g^{-1} catalyst in 10 wt.% $NaBH_4$ + 1 wt.% NaOH solution. Multiwalled carbon nanotube supported Co-B catalyst exhibited an average hydrogen generation rate of 5.10 l min^{-1} g^{-1} Co-B catalyst in 20 wt.% $NaBH_4$ + 3 wt.% NaOH solution [19]. Xu et al. [14] reported that activated carbon-supported $Co(OH)_2$ catalyst exhibited an average hydrogen generation rate of 0.53 l min^{-1} g^{-1} $Co(OH)_2$ catalyst in 1 wt.% $NaBH_4$ + 5 wt.% NaOH solution. It is also reported that an average hydrogen generation rate of 1.11 l min^{-1} g^{-1} Co catalyst was obtained using Co/γ-Al_2O_3 catalyst in 1 wt.% $NaBH_4$ + 5 wt.% NaOH solution [21]. In the present work, Co-B/AT catalysts produce an average hydrogen generation rate of 1.42 l min^{-1} g^{-1} Co-B catalyst in 5 wt.% $NaBH_4$ + 2 wt.% NaOH solution and 3.35 l min^{-1} g^{-1} Co-B catalyst in 5 wt.% $NaBH_4$ + 10 wt.% NaOH solution. Therefore, Co-B/AT catalyst is a promising catalyst with a high catalytic activity.

3.4. Effects of reacting temperature

Fig. 5 shows the effects of reacting temperature on the hydrogen generation rate in the 5 wt.% $NaBH_4$ + 2 wt.% NaOH solution. It can be seen clearly that increasing reacting temperature accelerates the hydrogen generation process. When the reacting temperature ranges from 20 °C to 40 °C, the reacting time declines from 24 min to 5 min.

The hydrogen generation rate of the zero-order hydrolysis reaction of $NaBH_4$, in the presence of clay-supported catalysts, can be calculated according to

$$r = \frac{d(V_{H_2})}{dt} = k_0 \cdot \exp\left(-\frac{E_a}{R} \cdot \frac{1}{T}\right) \quad (4)$$

where r is the hydrogen generation rate (l min^{-1} g^{-1} Co-B) in $NaBH_4$ hydrolysis reaction, V_{H_2} is the volume of generated hydrogen for

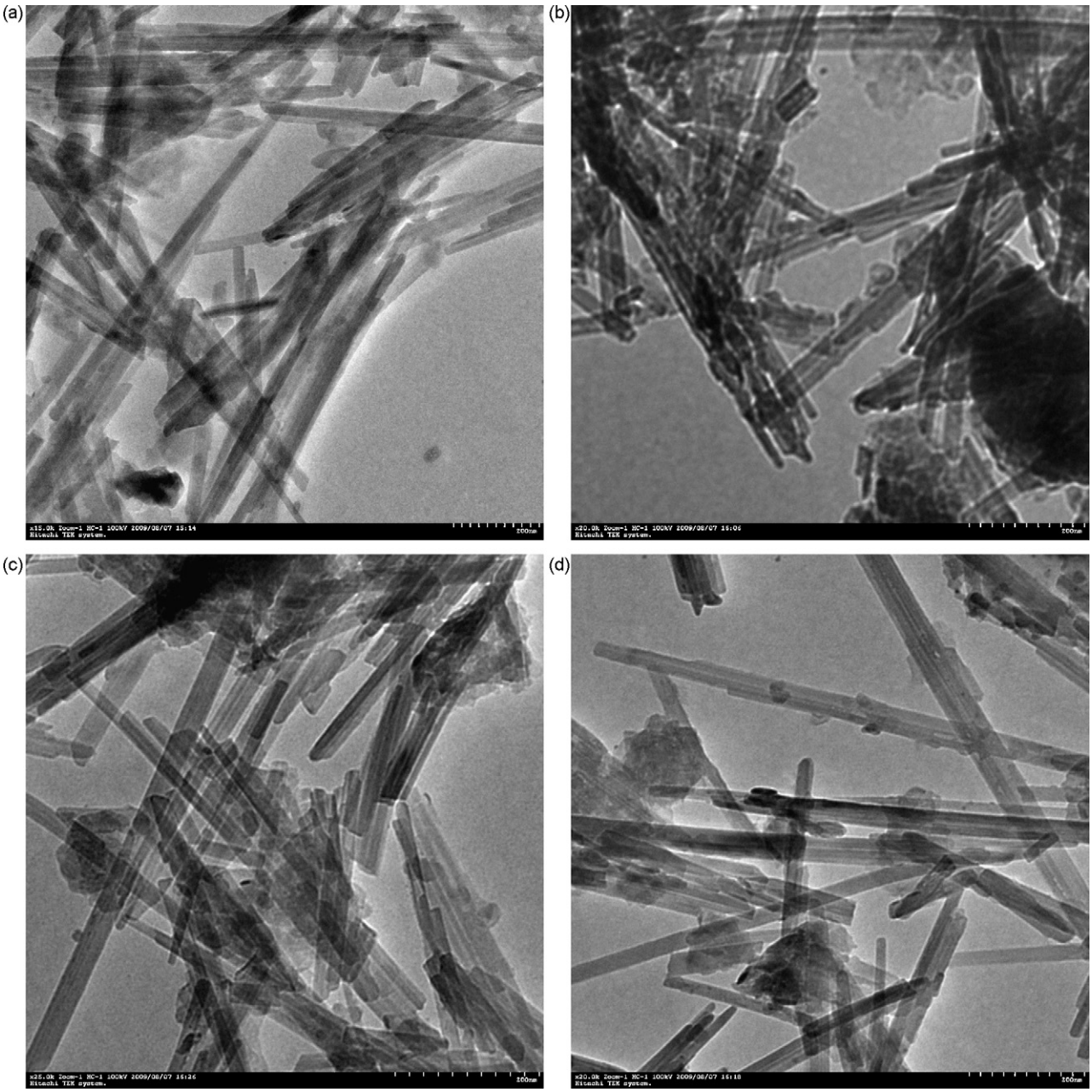

Fig. 10. Transmission electron micrographs of (a) fresh attapulgite clay without supported Co-B catalysts before the recycle test; (b) the catalysts after the 1st recycle test; (c) the catalysts after the 5th recycle test and (d) the catalysts after the 9th recycle test.

1 g Co-B catalyst ($l\,g^{-1}$ Co-B) at a certain time, t is the reacting time (min), k_0 is the apparent reaction constant, E_a is the activation energy ($kJ\,mol^{-1}$) for $NaBH_4$ hydrolysis reaction, R is the universal gas constant and T is the reacting temperature (K).

Following Eq. (4), $\ln r$ versus $1/T$ is plotted in Fig. 6. The slope of the straight line represents the value of activation energy and it is deduced to be 56.32 $kJ\,mol^{-1}$. This value compares favorably with the reported results for Co-B catalyst (64.87 $kJ\,mol^{-1}$) [12], Ni-Co-B catalyst (62.00 $kJ\,mol^{-1}$) [15], Co-P catalyst (60.20 $kJ\,mol^{-1}$) [5] and carbon-supported Co-B catalyst (57.80 $kJ\,mol^{-1}$) [20]. Table 3 provides a comparison of the value of activation energy in this work with some other published values. Although the value of the activation energy for clay-supported Co-B catalyst is relatively higher than the results for Co-B catalyst electrodeposited on Ni-foam (33.00 $kJ\,mol^{-1}$) [28], multiwalled carbon nanotubes supported Co-B catalysts (40.40 $kJ\,mol^{-1}$) [19], activated carbon-supported metallic Co catalyst (45.64 $kJ\,mol^{-1}$) [21] and zeolite-confined Ru nanocluster catalyst (49.00 $kJ\,mol^{-1}$) [24], its high catalytic activity, low cost and simple preparation method are very attractive in developing of PEM fuel cells.

3.5. Effects of recycle times

Fig. 7 highlights the effects of recycle times of the catalyst on the hydrogen generation rate in the recycle test. The test was carried out in 10 ml 10 wt.% $NaBH_4$ + 5 wt.% NaOH solution at 25 °C. The amount of the clay-supported catalyst was 0.5 g.

From Fig. 7, it can be observed that from the 1st cycle to the 9th cycle the average hydrogen generation rate decreases gradually from 1.27 $l\,min^{-1}\,g^{-1}$ Co-B to 0.87 $l\,min^{-1}\,g^{-1}$ Co-B. This may be caused by two reasons. One, the losses of catalyst particles in the filtration and washing process. And two, some by-products including sodium metaborate ($NaBO_2$), borax ($Na_2B_4O_7{\cdot}10H_2O$), potassium borate (KB_xO_y), boron oxide (B_2O_3) and so on [20,21], may cover the catalyst surface and reduce the catalytic reactivity of the catalysts.

3.6. Characterization of catalysts before and after recycle tests

Structural characterizations of the catalysts before and after the recycle test were examined by a D8 Advance X-ray diffractometer using the Cu Kα radiation (the angle in the range between 10° and 90° and with a step of 0.05°) operating at 40 kV and 50 mA. Scanning electron microscopy (SEM) analyses were carried out with a JEOL JSM-6700F microscope. Transmission electron microscopy (TEM) analyses were also performed using a HITACHI H-700 microscope that operates at an accelerating voltage of 200 kV.

Fig. 8 shows the XRD patterns of the attapulgite clay-supported catalysts after the 1st recycle test, the 5th recycle test and the 9th recycle test. Such XRD patterns reveal that the presence of crystalline SiO_2 at $2\theta = 27°$ in all the three catalysts as the only clearly identified chemical compound in the catalysts. It is also indicated in Fig. 8 that the produced Co-B components is completely amorphous because no distinct peak is observed.

Figs. 9 and 10 present SEM images and TEM images, respectively, of the fresh attapulgite clay powders, the catalyst powders after the 1st cycle, after the 5th cycle and after the 9th cycle. It is shown in Figs. 9(a) and 10(a) that the long and narrow rod-shape attapulgite clay particle aggregates together unorderly forming some fibrous bundles. As shown in Fig. 10(b), the Co-B catalyst particles are well disturbuted in the surface of the clay particles after the 1st cycle. As the recycle test proceeds, as shown in Figs. 9(c) and 10(c), some aggregations are broke up into separated fibrous particles. Accordingly, the "channels" in the aggregations are destroyed gradually. After the 9th-cycle utilization, it can be observed in Figs. 9(d) and 10(d) that there are only a few aggregations in the residues.

4. Conclusion

The attapulgite clay-supported Co-B catalysts are developed by a simple impregnation reduction method. The cost of the prepared catalysts is quite low and the catalysts show high catalytic activity and good recyclability in hydrogen generation process. High NaOH concentration, big catalyst amount and high reacting temperature are all beneficial to improve the hydrogen generation rate. Besides, there is an optimum range for $NaBH_4$ concentration, around 15 wt.%, to promote hydrogen generation rate. In the recycle tests of the catalysts, from the 1st cycle to the 9th cycle, the hydrogen generation rate decreases gradually from 1.27 $l\,min^{-1}\,g^{-1}$ Co-B to 0.87 $l\,min^{-1}\,g^{-1}$ Co-B. The value of activation energy for the hydrogen generation process is calculated to be 56.32 $kJ\,mol^{-1}$ and it compares favorably with some other previously reported values.

Acknowledgements

The financial support from New Century Excellent Talents in University (NCET-07-0473), from Natural Science Foundation of China (20676064, 20876079), and Taishan Mountain Scholar Constructive Engineering Foundation (JS 200510036), is greatly appreciated.

References

[1] International energy agency, Energy Technology Perspectives: Scenarios and Strategies to 2050, Group of Eight (G8) Summit, Gleneagles, July 2005.
[2] J. Butler, Report on the Survey of Portable Fuel Cell in 2009, Fuel cell today, 2009, http://www.fuelcelltoday.com/online/survey?survey=2009-05/2009-Portable-Chinese (accessed August 2009).
[3] S.C. Amendola, S.L. Shap-Goldman, M.S. Janjua, M.S. Janjua, N.C. Spencer, M.T. Kelly, P.J. Petillo, M. Blinder, Int. J. Hydrogen Energy 25 (2000) 969–975.
[4] B.H. Liu, Q. Li, Int. J. Hydrogen Energy 33 (2008) 7385–7391.
[5] K. Eom, K.W. Cho, H.S. Kwon, J. Power Sources 180 (2008) 484–490.
[6] S. Özkar, M. Zahmakiran, J. Alloys. Compd. 404–406 (2005) 728–731.
[7] J.H. Park, P. Shakkthivel, H.J. Kim, M.K. Han, J.H. Jang, Y.R. Kim, Int. J. Hydrogen Energy 33 (2008) 1845–1852.
[8] N. Patel, B. Patton, C. Zanchetta, R. Fernades, G. Guella, A. Kale, Int. J. Hydrogen Energy 33 (2008) 287–292.
[9] S.F. Yin, Q.H. Zhang, B.Q. Xu, W.X. Zhu, C.F. Ng, C.T. Au, J. Catal. 224 (2004) 384–389.
[10] Y. Kojima, K. Suzuki, K. Fukumoto, M. Sasaki, T. Yamamoto, Y. Kawai, Int. J. Hydrogen Energy 27 (2002) 1029–1034.
[11] H. Dong, H. Yang, X. Ai, C. Cha, Int. J. Hydrogen Energy 28 (2003) 1095–1100.
[12] S.U. Jeong, R.K. Kim, E.A. Cho, H.J. Kim, S.W. Nam, I.H. Oh, S.A. Hong, S.H. Kim, J. Power Sources 144 (2005) 129–134.
[13] C. Wu, F. Wu, Y. Bai, B.L. Yi, H.M. Zhang, Mater. Lett. 59 (2005) 1748–1751.
[14] D. Xu, P. Dai, X. Liu, C. Cao, Q. Guo, J. Power Sources 182 (2008) 616–620.
[15] J.C. Ingersoll, N. Mani, J.C. Thenmozhiyal, A. Muthaiah, J. Power Sources 173 (2007) 450–457.
[16] D.R. Kim, K.W. Cho, Y.I. Choi, C.J. Park, Int. J. Hydrogen Energy 34 (2009) 2622–2630.
[17] R. Fernades, N. Patel, A. Miotello, Int. J. Hydrogen Energy 34 (2009) 2893–2900.
[18] L. Huang, X. Jian, C. Wei, R. Chen, D. Chu, T.H. Andrew, Catal. Commun. 10 (2009) 502–508.
[19] Y. Huang, Y. Wang, R. Zhao, P.K. Shen, Z. Wei, Int. J. Hydrogen Energy 33 (2008) 7110–7115.
[20] J. Zhao, H. Ma, J. Chen, Int. J. Hydrogen Energy 32 (2007) 4711–4716.
[21] W. Ye, H. Zhang, D. Xu, L. Ma, B. Yi, J. Power Sources 164 (2007) 544–548.
[22] O. Metin, S. Ozkar, Energy Fuel 23 (2009) 3517–3526.
[23] C.H. Liu, B.H. Chen, C.L. Hsueh, J.R. Ku, M.S. Jeng, F. Tsau, Int. J. Hydrogen Energy 34 (2009) 2153–2163.
[24] M. Zahmakiran, S. Ozkar, Langmuir 25 (2009) 2667–2678.
[25] C.L. Hsueh, C.Y. Chen, J.R. Ku, S.T. Tsai, Y.Y. Hsu, F. Tsau, M.S. Jeng, J. Power Sources 177 (2008) 485–492.
[26] J.M. Lu, D.B. Dreisinger, W.C. Copper, Hydrometallurgy 45 (1997) 305–322.
[27] P. Krishnan, T.H. Yang, W.Y. Lee, C.S. Kim, J. Power Sources 143 (2005) 17–23.
[28] H.B. Dai, Y. Liang, P. Wang, H.M. Cheng, J. Power Sources 177 (2008) 17–23.
[29] C. Wu, Y.B.F. Wu, Mater. Lett. 62 (2008) 4242–4244.